Electronic Supplementary Material (ESI) for Reaction Chemistry & Engineering.
This journal is © The Royal Society of Chemistry 2023

Supplementary Information

Table of Contents

S1 Synthesis methods and characterisation

S1.1 General Methods

Unless otherwise stated, materials were purchased from commercial sources and used as received without further purification. Acetone was dried over 3 Å molecular sieves in a solvent purification system. Automated flash column chromatography was performed using a Teledyne ISCO CombiFlash NextGen 100 system using pre-packed silica columns with a gradient of petroleum ethers/ethyl acetate. Microwave heating was performed in a Biotage Initiator microwave reactor at high absorption level.

^{1}H and ^{13}C NMR spectra were recorded on Bruker AVANCE III HD spectrometers (400 MHz for ^{1}H NMR; 101 MHz for ^{13}C NMR). ^{1}H NMR chemical shifts (δ_H) and ^{13}C NMR chemical shifts (δ_C) are quoted in parts per million (ppm) downfield of tetramethylsilane (TMS) and reported relative to residual solvent peaks ($CDCl_3$: δ_H = 7.26 ppm and δ_C = 77.16 ppm).

No unexpected or unusually high safety hazard were encountered.

S1.2 Synthesis of 4-methoxy phenyl ally ether (1a)

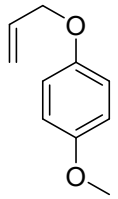

In a 500 mL RB flask fitted with a reflux condenser, a solution of 4-methoxyphenol (10.1 g, 81.4 mmol) in acetone (250 mL) was stirred at 300 rpm. Potassium carbonate (22.3 g, 161 mmol) was added in batches and the solution was heated to 60 °C under nitrogen and left to stir for 20 minutes. Allyl bromide (9.80 g, 81.0 mmol) was then added and the solution was heated to reflux (66 °C) and left to stir for 4 hours. After cooling to ambient temperature, the solution was filtered through celite and evaporated *in vacuo*. The residue was purified by automated column chromatography in 10% ethyl acetate in petroleum ether. This produced the desired product as a colourless oil (9.05 g, 44.8 mmol, 55%).

^{1}H NMR (400 MHz, $CDCl_3$) δ 6.93 – 6.78 (m, 4H), 6.23 – 5.89 (m, 1H), 5.58 – 5.13 (m, 2H), 4.65 – 4.35 (m, 2H), 3.77 (s, 3H). ^{13}C NMR (101 MHz, $CDCl_3$) δ 153.97, 152.81, 133.70,

117.58, 115.78, 114.67, 69.58, 55.78. These data are consistent with the reported literature values.[1]

S1.3 Synthesis of starting materials in medium throughput (1b, 1c, 1e, 1f, 1g, 1h)

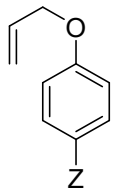

The precursors were prepared in parallel using a Reactarray Barnstead RAR-010A reaction station equipped with 10 x 25 mL reactors that are fitted individually with reflux condensers. Each reactor was flushed with N_2 and charged with a cross-shaped stirrer, potassium carbonate (2.50 g, 18.1 mmol), the requisite phenol starting material (approximately 6 mmol., see table S1 for quantities) and dry acetone (20 mL). The reaction mixtures were subsequently stirred with gentle heating at 30 °C for 20 minutes in order to ensure deprotonation of the phenol. Allyl bromide (1.13 g, 9.34 mmol) was added to each reactor *via* a pipette, and the reaction mixtures were left stirring at 30 °C for 18 hours. After cooling, the solutions were filtered through celite into falcon tubes and the acetone was removed using a nitrogen blow down evaporator. This produced the desired products as listed below in Table S1.

Table S1. Values for the medium throughput synthesis of para substituted phenyl allyl ether **1**.

Compound	Z	MW of phenol / g mol^{-1}	mass of phenol / g	mass of 1x / g	isolated yield / %	Description
1b	Me	108.14	0.655	0.656	73	orange oil
1c	F	112.10	0.336	0.360	79	colourless oil
1e	C(O)CH$_3$	136.15	0.817	0.956	91	colourless oil
1f	CN	119.12	0.752	0.705	70	white solid
1g	NHAc	151.16	0.907	0.915	80	white solid
1h	Br	173.01	1.03	1.09	87	colourless oil

1b (Z = Me):

^{1}H NMR (400 MHz, $CDCl_3$) δ 7.08 (d, *J* = 8.2 Hz, 2H), 6.83 (d, *J* = 8.2 Hz, 2H), 6.23 – 5.94 (m, 1H), 5.56 – 5.13 (m, 2H), 4.62 – 4.39 (m, 2H), 2.29 (s, 3H). ^{13}C NMR (101 MHz, $CDCl_3$) δ 156.59, 133.66, 130.18, 130.00, 117.65, 114.71, 69.02, 20.61. These data are consistent with the reported literature values.[2]

1c (Z = F):

^{1}H NMR (400 MHz, $CDCl_3$) δ 7.06 – 6.81 (m, 4H), 6.17 – 5.94 (m, 1H), 5.67 – 5.09 (m, 2H), 4.58 – 4.47 (m, 2H). ^{13}C NMR (101 MHz, $CDCl_3$) δ 157.43 (d, *J* = 238.4 Hz), 154.82, 133.31, 117.91, 115.96 (d, *J* = 12.7 Hz), 115.81 (d, *J* = 2.5 Hz), 69.56. These data are consistent with the reported literature values.[2]

1e (Z = $C(O)CH_3$):

^{1}H NMR (400 MHz, $CDCl_3$) δ 7.92 (d, *J* = 8.3 Hz, 2H), 6.94 (d, *J* = 8.3 Hz, 2H), 6.19 – 5.95 (m, 1H), 5.50 – 5.25 (m, 2H), 4.64 – 4.56 (m, 2H), 2.55 (s, 3H). ^{13}C NMR (101 MHz, $CDCl_3$) δ 196.91, 162.59, 132.60, 130.69, 130.54, 118.34, 114.50, 69.00, 26.49. These data are consistent with the reported literature values.[3]

1f (Z = CN):

^{1}H NMR (400 MHz, $CDCl_3$) δ 7.57 (d, *J* = 8.3 Hz, 2H), 6.95 (d, *J* = 8.3 Hz, 2H), 6.10 – 5.95 (m, 1H), 5.49 – 5.27 (m, 2H), 4.63 – 4.53 (m, 2H). ^{13}C NMR (101 MHz, $CDCl_3$) δ 161.93, 134.07, 132.16, 119.31, 118.61, 115.55, 104.17, 69.10. Melting point: 44 – 46 ℃. These data are consistent with the reported literature values.[4]

1g (Z = NHAc):

^{1}H NMR (400 MHz, $CDCl_3$) δ 7.42 – 7.33 (m, 2H), 7.19 (s, 1H), 6.91 – 6.81 (m, 2H), 6.15 – 5.95 (m, 1H), 5.46 – 5.23 (m, 2H), 4.54 – 4.47 (m, 2H), 2.15 (s, 3H). ^{13}C NMR (101 MHz, $CDCl_3$) δ 168.33, 155.57, 133.36, 131.21, 121.96, 117.86, 115.18, 69.22, 24.52. Melting point: 95 – 97 ℃. These data are consistent with the reported literature values.[5]

1h (Z = Br):

^{1}H NMR (400 MHz, $CDCl_3$) δ 7.37 (d, *J* = 8.3 Hz, 2H), 6.80 (d, *J* = 8.3 Hz, 2H), 6.10 – 5.96 (m, 1H), 5.46 – 5.25 (m, 2H), 4.54 – 4.48 (m, 2H). ^{13}C NMR (101 MHz, $CDCl_3$) δ 157.80, 132.98, 132.37, 118.08, 116.68, 113.12, 69.12. These data are consistent with the reported literature values.[6]

S1.4 Synthesis of 2-allyl-4-methoxy phenol (2a)

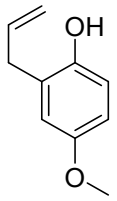

4-Methoxy phenyl allyl ether (**1a**, 1.60 g, 9.75 mmol) was added to a 0.5 – 2 mL microwave vial with a stirrer. The vial was subjected to microwave heating at 200 °C for 40 min. After cooling to room temperature, the crude product formed was dissolved in petroleum ether (10 mL) and extracted into a 2.5 M NaOH solution (2 x 5 mL). The combined aqueous layers were washed with petroleum ether (2 x 5 mL) before re-acidifying - with conc. HCl (6 mL) to pH 2. The acidified aqueous layer was extracted with ethyl acetate (3 x 10 mL). The combined ethyl acetate washes were diluted with petroleum ether (40 mL) and filtered through a silica plug. The organic mixture was dried over magnesium sulfate, filtered and evaporated *in vacuo* to produce the desired product as a pale yellow oil (1.33 g, 8.11 mmol, 83%).

^{1}H NMR (400 MHz, $CDCl_3$) δ 6.81 – 6.60 (m, 3H), 6.13 – 5.90 (m, 1H), 5.20 – 5.09 (m, 2H), 4.55 (br s, 1H), 3.76 (s, 3H), 3.45 – 3.29 (m, 2H). ^{13}C NMR (101 MHz, $CDCl_3$) δ 153.92, 148.10, 136.28, 126.54, 116.73, 116.64, 116.06, 112.76, 55.86, 35.50. These data are consistent with the reported literature values.[7]

S1.5 Synthesis of other aromatic Claisen products (2b-h)

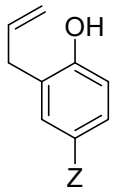

2d-f:

200 µL of each allyl ethers (**1d-f**) were dissolved in 9 mL ethanol and 5 mL of water using a pipette in quantities listed below in Table S2. The solutions were then pumped through the flow system at 0.2 mL min^{-1} at 220 °C (16 min residence time). Prior to each experiment, the system was primed with the reaction solution for 2 min at 1 mL min^{-1} and the reactor was heated to 220 °C. The reaction solution was pumped at 0.2 mL min^{-1} at 70 bar for 23 min.[1] The reactor effluent was then collected for 70 min with addition of ethanol to the inlet at 35 min. After each experiment the system was then flushed with ethanol. Each solution was evaporated to half volume *in vacuo* to remove the ethanol. The resultant solution was dissolved in DCM (10 mL)

[1] The time taken for solution to pass from the mixer to the outlet of the system.

and 2.5 M NaOH (10 mL) was added. The separated aqueous solution was acidified with 2 M HCl (15 – 25 mL) and washed with DCM (10 mL). The DCM was evaporated *in vacuo* to afford the desired products.

2b:

Attempts to produce **2b** (Z = Me) by the above method failed to furnish clean products even after flash column chromatography, as the product either appeared to either remain on the column (silica or alumina) or degrade. Hence, the Claisen rearrangement of **1b** (0.281 g) was performed in flow, by dissolving the precursor in DMF (10 mL) and subjected to heating at 240 °C using the flow system for 4 hours (recirculatory mode, 0.5 mL min^{-1}). Diethyl ether (20 mL) was then added, and the resultant solution was washed with saturated lithium chloride solution (5 x 20 mL). The diethyl ether was then evaporated to give the desired product as a pale yellow oil (0.205 g, 1.38 mmol, 73%)

2c and **2g**:

200 µL of allyl ether **1c** or **1g** were dissolved in ethanol (20 mL) in quantities listed below in Table S2. The reaction solution was subjected to heating at 250 °C using the flow system for 1 hours (recirculatory mode, 0.5 mL min^{-1}). The ethanolic solution is then collected and evaporated *in vacuo*. The residue is dissolved in DCM (10 mL) and 2.5 M NaOH (10 mL) was added. The separated aqueous solution was acidified with 2 M HCl (25 mL) and washed with DCM (10 mL). The DCM was evaporated *in vacuo* to afford the desired products.

Table S2. Values for the medium throughput synthesis of aromatic Claisen products **2**.

Compound	Z	mw of SM / g mol^{-1}	mass of 1 / g	mass of 2 / g	isolated yield / %	Description
2b	Me	148.09	0.281	0.205	73	Orange oil
2c	F	152.06	0.055	0.049	89	Orange oil
2d	H	134.07	0.283	0.116	41	Colourless oil
2e	$C(O)CH_3$	176.08	0.313	0.157	50	White solid
2f	CN	159.07	0.166	0.132	80	White solid
2g	NHAc	191.09	0.182	0.164	95	White solid
2h	Br	211.98	0.418	0.197	47	White solid

2b (Z = Me):

^{1}H NMR (400 MHz, $CDCl_3$) δ 6.99 – 6.88 (m, 2H), 6.77 – 6.66 (m, 1H), 6.16 – 5.94 (m, 1H), 5.31 – 5.08 (m, 2H), 4.86 (s, 1H), 3.43 – 3.34 (m, 2H), 2.27 (s, 3H). ^{13}C NMR (101 MHz, $CDCl_3$) δ 151.96, 136.68, 131.10, 130.25, 128.38, 125.14, 116.47, 115.79, 35.29, 20.61. These data are consistent with the reported literature values.[7]

2c (Z = F):

^{1}H NMR (400 MHz, $CDCl_3$) δ 7.05 – 6.65 (m, 3H), 6.08 – 5.90 (m, 1H), 5.26 – 5.09 (m, 2H), 4.76 (br s, 1H), 3.43 – 3.33 (m, 2H). ^{13}C NMR (101 MHz, $CDCl_3$) δ 158.49, 156.12, 150.09, 135.67, 127.02, 117.21, 116.92, 116.74, 116.69, 116.65, 116.38, 116.30, 116.24, 116.01, 114.19, 113.96, 35.14. NB: some of the ^{13}C shifts are doublets caused by coupling to ^{19}F. These data are consistent with the reported literature values.[8]

2d (Z = H):

^{1}H NMR (400 MHz, $CDCl_3$) δ 7.19 – 7.07 (m, 2H), 6.94 – 6.86 (m, 1H), 6.86 – 6.78 (m, 1H), 6.11 – 5.96 (m, 1H), 5.21 – 5.12 (m, 2H), 4.96 (br s, 1H), 3.51 – 3.29 (m, 2H). ^{13}C NMR (101 MHz, $CDCl_3$) δ 154.23, 136.52, 130.58, 128.05, 125.40, 121.10, 116.63, 115.95, 35.27. These data are consistent with the reported literature values.[9]

2e (Z = $C(O)CH_3$):

^{1}H NMR (400 MHz, $CDCl_3$) δ 7.85 – 7.75 (m, 2H), 6.97 – 6.84 (m, 1H), 6.09 – 5.94 (m, 1H), 5.23 – 5.07 (m, 2H), 3.52 – 3.40 (m, 2H), 2.57 (s, 3H). ^{13}C NMR (101 MHz, $CDCl_3$) δ 198.25, 159.37, 135.86, 131.52, 130.13, 129.38, 126.08, 116.99, 115.64, 34.83, 26.45. Melting point: 113 – 114 °C. These data are consistent with the reported literature values.[10]

2f (Z = CN):

^{1}H NMR (400 MHz, $CDCl_3$) δ 7.48 – 7.40 (m, 1H), 7.18 – 6.79 (m, 2H), 6.10 – 5.89 (m, 1H), 5.34 – 5.09 (m, 2H), 3.46 – 3.37 (m, 2H). ^{13}C NMR (101 MHz, $CDCl_3$) δ 158.07, 134.93, 134.65, 132.55, 130.59, 117.98, 116.65, 104.43, 34.61. Melting point: 80 – 82 °C. These data are consistent with the reported literature values for NMR shifts[7] and melting point.[11]

2g (Z = NHAc):

^{1}H NMR (400 MHz, $CDCl_3$) δ 7.25 – 7.17 (m, 2H), 7.10 (br s, 1H), 6.81 – 6.69 (m, 1H), 6.07 – 5.90 (m, 1H), 5.19 – 5.11 (m, 2H), 3.48 – 3.31 (m, 2H), 2.14 (s, 3H). ^{13}C NMR (101 MHz, $CDCl_3$) δ 168.53, 151.36, 136.22, 130.85, 126.15, 123.09, 120.60, 116.83, 116.23, 35.16, 24.48. Melting point: 94 – 96 °C. No literature values have been reported for NMR shifts.[12]

2h (Z = Br):

^{1}H NMR (400 MHz, $CDCl_3$) δ 7.32 – 7.17 (m, 2H), 6.75 – 6.64 (m, 1H), 6.09 – 5.85 (m, 1H), 5.29 – 5.08 (m, 2H), 4.93 (br s, 1H), 3.42 – 3.31 (m, 2H). ^{13}C NMR (101 MHz, $CDCl_3$) δ

153.37, 135.60, 133.12, 130.72, 127.78, 117.67, 117.35, 113.03, 34.95. Melting point: 58 – 60 ℃. These data are consistent with the reported literature values for NMR shifts[6] and melting point.[12]

S2 Flow system

S2.1 Flow system overview

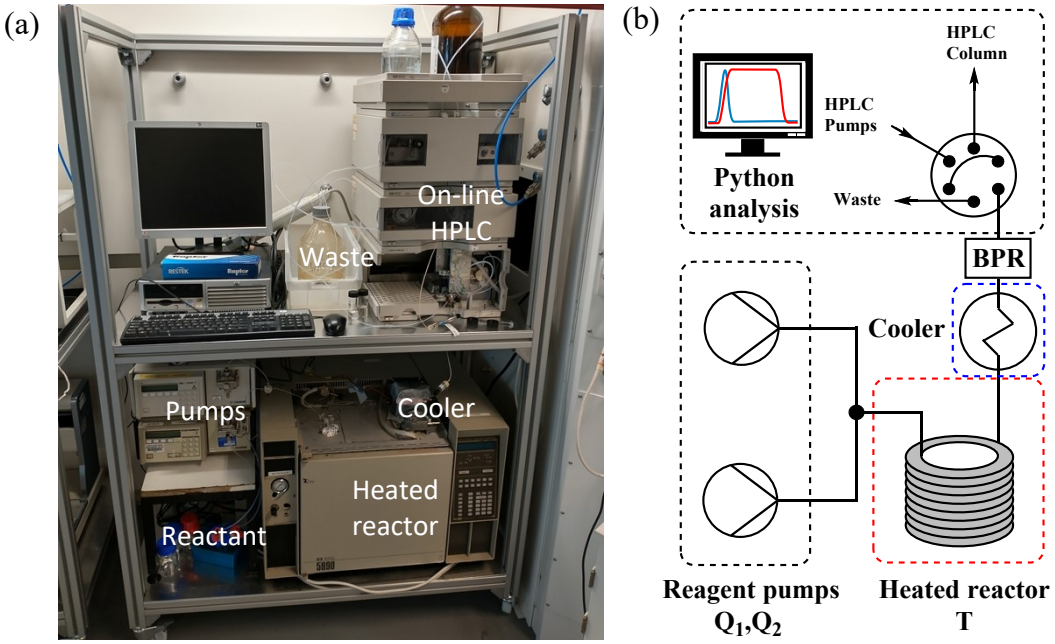

Figure S1. (a) the flow system utilised in this work; (b) a schematic representation of the fluidic path and key components of the flow system.

A flow system (Fig. S1) was constructed in which reagent(s) and solvent(s) as solutions are delivered from Duran bottles fitted with inlet tubing with in-line filters. The inlet tubing lines (1/8" OD, 2 mm ID PTFE, 1.6 mL and 1.2 mL respectively) were connected to a Gilson 305 HPLC pump (pump A) and a Gilson 307 HPLC pump (pump B) respectively. The outlets of these pumps were connected to two stainless steel tubing (25 cm) which fed into a Valco T-piece stainless steel mixer. For collection of experimental data for this work only one pump was used, but both pumps were used to calibrate the on-line HPLC (see S2.4).

The outlet of the mixer is connected to a 5.14 m length of stainless steel tubing (1 mm ID, 1/16" OD); the first 30 cm of which are outside of the GC oven (heated reactor length: 4.84 m, heated reactor volume: 3.92 mL). This is then connected by a stainless steel HPLC style union at the outlet of the GC oven through an insulating PTFE sheet to a length of stainless steel tubing (14 cm) which passes through a custom built cooling system consisting of an aluminium block and a Peltier assembly. The outlet of the cooling device is connected by a stainless steel HPLC style union to a 20 cm length of stainless steel tubing into a VALCO variable pressure

BPR. The BPR outlet is connected to a 25 cm length of stainless steel tubing which connects to the modified HPLC 6-port, 2-way injector valve.

This flow system is a modification of a system previously used in our lab which was previously thoroughly assessed for residence time distributions.[13]

S2.2 Pumps

The pumps used are a Gilson 305 HPLC pump and a Gilson 307 HPLC pump with a 10 mL WSC and 10 mL SC pump heads respectively. The inlet and outlet fittings to the Gilson pumps are standard Gilson 30X fittings. All other fittings are HPLC style fittings. These are connected by a GSIOC cable to allow pump control through the inbuilt Gilson firmware. The pressure of the system is monitored by the manometric module in the Gilson 307 pump. In order to maintain the pumps in working order and confirm their accuracy, the check valves are cleaned and sonicated in methanol regularly, and the cumulative flow rate of the system is confirmed at different flow rates and at different times during experimentation.

S2.3 Heating and cooling

Heating is performed by an HP 5890 Series II GC oven, using the inbuilt software/PID to allow accurate control over temperature ramping. Cooling is performed by a 60 W Peltier thermo-electric cooler module and heatsink assembly (PiHut) with a custom cooling block milled to fit 1/16" tubing by the Advanced HackSpace, Imperial College London.

S2.4 On-line HPLC

On-line analysis was implemented by modifying the injector on an Agilent HP 1100 series HPLC. The fittings to the 6-port, 2-way injector valve were disconnected and reconnected as shown in the scheme above to allow a 1.8 μL sample loop to be continually filled from the reactor effluent in the resting valve position. When triggered by the Chemstation HPLC software the injector method switches the valve to its second position for 0.1 min, allowing the contents of the sample loop to be redirected by solvent from the Agilent HP 1100 series pumps into the column and subsequent detector.

HPLC method

The column used was a Restek Raptor C18 2.7μm 50 mm x 2.1 mm running a gradient method in water and acetonitrile as described in Table S3. In the method, the time after the gradient allowed the column to re-equilibrate to a steady state pressure before the following injection. This method allowed injections every 6.5 minutes.

Table S3. Key parameters set for the HPLC method used in this work for on-line HPLC analysis.

Flow rate / mL min^{-1}	0.7
Stoptime / min	5.75
Posttime / min	0.29
Solvent A	H_2O
Solvent B	MeCN
DAD wavelength / nm	210

Time / min	**%B**
0	25
1.2	30
3.5	50
3.51	60
3.85	60
3.86	25

The Agilent 1100 Autosampler 1 automatically switches the valve at the beginning of the injector program. The inputted injector cycle is a "WAIT" command for 0.10 min and then a "VALVE MAINPASS" command.

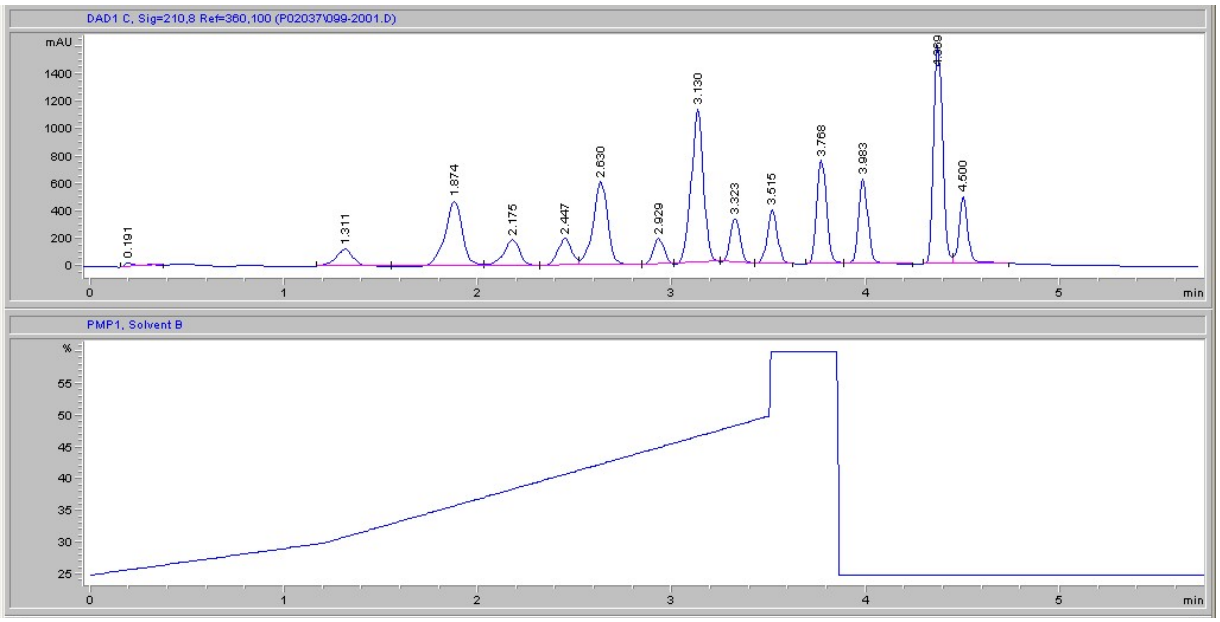

Figure S2. An example chromatogram of a "one-pot" method using the HPLC method discussed above. The lower diagram shows a diagrammatic representation of the HPLC method.

Table S4. Substituents for phenyl allyl ether substrates and their corresponding retention times in the HPLC method in Figure S2.

1/2	Z	Retention time of 1/ min	Retention time of 2/ min
a	*p*-MeO	3.52	1.87
b	*p*-Me	4.50	3.32
c	*p*-F	3.98	2.93
d	H	3.77	2.45
e	*p*-C(O)CH_3	2.63	1.31
f	*p*-CN	3.13	2.18
-	ethyl benzene	4.39	

Calibration method

The HPLC method was used to determine quantitative concentrations of starting materials and products by generating calibration curves based on known concentration samples. Starting material and product peak areas were measured relative to the area of the internal standard peak (ethyl benzene). Ethyl benzene was chosen as a non-interacting internal standard that is UV visible, thermally stable, stable to solvolysis and separable from the starting materials and products by liquid chromatographical methods.

Multiple solutions were prepared, using pipettes and volumetric flasks, containing varying quantities of ethyl benzene and allyl phenyl ether. Dilutions of these solutions were injected into the HPLC in a manual method to give 5 point calibration curves. Another method was also used for calibration by which a solution containing a substrate or product at a known concentration in ethanol was pumped through the flow system, with simultaneous delivery of a solution of ethyl benzene in ethanol by the second pump (Fig. S3). By varying the ratio of flow rates of the two pumps in a linear manner, whilst maintaining the same cumulative flow rate, it was possible to generate calibration curves with greater than 10 calibration points each using our on-line HPLC setup. In order to further improve this process, we found it was possible and expedient to calibrate multiple substrates at a time using this method and thus accurate dense calibration curves could be generated rapidly.

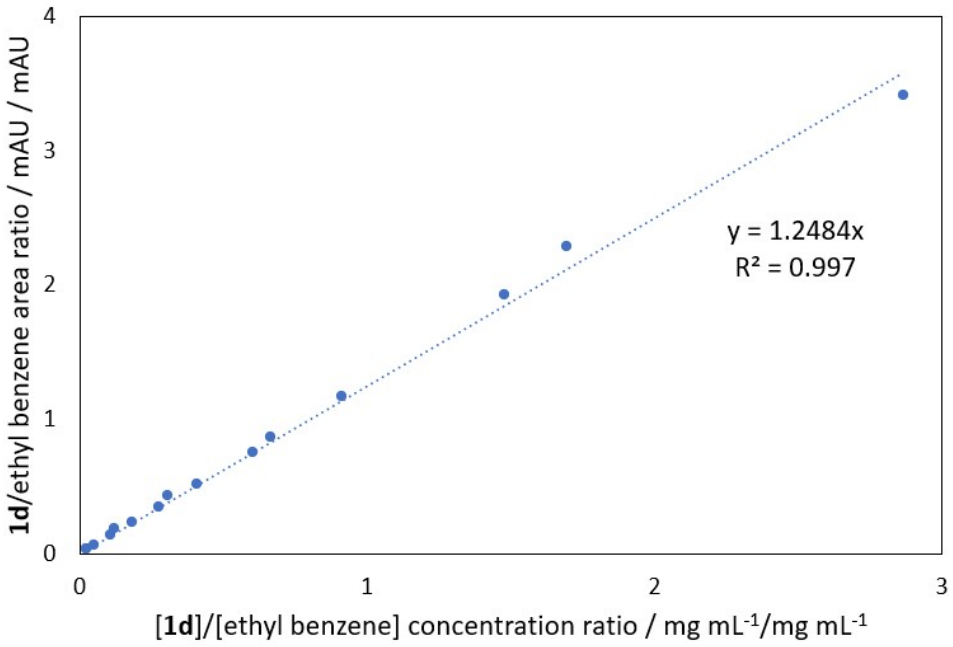

Figure S3. An example HPLC calibration curve collected *via* a flow rate ramp between a solution containing starting materials including **1d (**Z = H) and a solution containing ethyl benzene as an internal standard.

S3 Transient flow experimental work

S3.1 Solution preparation for flow experiments

Solutions were made for the flow experiments by pipetting 40 μL of ethyl benzene (as an internal standard) into a vial and noting the mass. This was then tared and the process repeated in the same vial with 30 μL of the given allyl phenyl ether **1** desired for the experiment. This was further repeated for the one pot experiments with further iterations was further allyl phenyl ethers.

The content of this vial was then washed into a volumetric flask (100 mL) with absolute ethanol, which was then made up to 100 mL with the addition of absolute ethanol. This solution was mixed thoroughly by inversions and then filtered through a 25 mm 0.45 μm pore PTFE syringe filter into a Duran bottle which had been carefully washed and dried to avoid particles being present. The solution was then attached to an inlet line on the flow system as described above.

S3.2 First order plots and validity of single time point method

The reaction was monitored at 200, 220, 240 °C at a flow rate range between 1 mL min^{-1} and 0.2 mL min^{-1} corresponding to residence times (τ) between 3 and 16 minutes whilst maintaining a back pressure between 95 and 105 bar to avoid pressure dependent fluctuations in solvent properties in the near critical region for ethanol. The method consisted of running the system

at 1 mL min^{-1} for 10 minutes and then having an automated step change of flow rate to 0.2 mL min^{-1} which was then held for 30 minutes. The temperature was then changed, and the method repeated.

At the temperatures investigated the reaction appears to be an ideal first order reaction as demonstrated by the linearity of a natural logarithm *vs*. time plot (Fig. S4a). The first order kinetics allowed us to take each point of our residence time ramps and determine a rate constant from it, similar to the initial rates method. This allowed us to monitor the error that we would expect if we were to only collect data at one residence time in the future to generate kinetic rate constants by comparing different single time point data to each other in an Arrhenius plot (Fig. S4b).

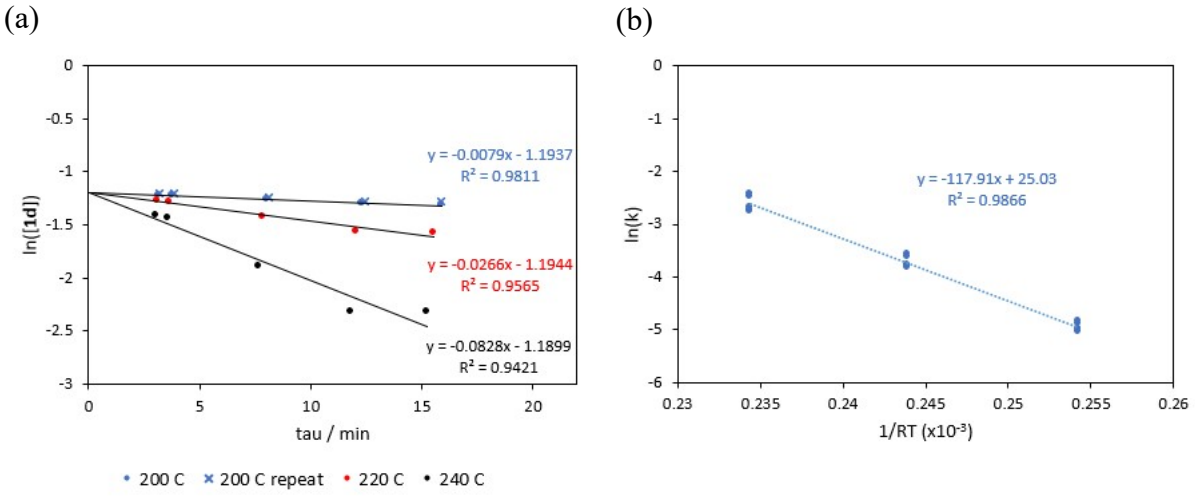

Figure S4. Data collected on the aromatic Claisen rearrangement of phenyl allyl ether (**1d**) *via* transient residence time step change methodology at three temperatures expressed as: (a) a first order kinetic plot; (b) an Arrhenius plot.

The activation energy can be obtained from the Arrhenius plot generated from these residence time ramps using data from all residence times (Fig. S4b). This corroborated the repeatability of this method for future use, highlighting the insensitivity of the calculated rate constant k to the residence time.

S3.3 Transient temperature ramp method

The data shown in Figure 2 were collected *via* transient temperature ramps. These were performed by priming the system at 2 mL min^{-1} for 4 minutes whilst heating the reactor to the desired initial temperature, controlled by the GC oven. The flow rate was then lowered to 0.2 mL min^{-1} and a temperature ramp was programmed into the GC oven and executed. This ramp varied in timings and temperatures but in general began with a 30 minute hold at the initial

temperature, then a ramp at a rate of 0.5 °C min^{-1} to achieve the final temperature which was then maintained for a further 30 minutes.

In order to confirm a lack of hysteresis in the system (differences in results from the order in which they are collected and how the conditions are implemented) temperature ramps were executed, in which in the same experimental run a ramp up to a temperature was followed by a ramp down over the same temperature range. These showed good consistency at a ramp rate of 0.5 °C min^{-1} whereas at a faster ramp rate of 1 °C min^{-1} this was not the case, as previously discussed by Jensen *et al.*.[14] Thus 0.5 °C min^{-1} was chosen as a good ramp rate for accuracy and data density.

The rate of ramping was also important for the analysis of our data. We calculated the average temperature that each sample experienced in the reactor and used this value as the temperature of reaction in the Arrhenius plots. If the ramp rate were too high this could cause issues due to the exponential dependency of the Arrhenius relationship on temperature. At a ramp rate of 0.5 °C min^{-1} each sample experienced a temperature range of 10 °C.

S3.4 Mass balance

Mass balance was calculated by dividing the sum of starting material **1** and product **2** concentrations by the initial starting material **1** concentration (Fig. S5). These were generally found to be between 95 and 110% although in some cases slight trending could be observed at increased temperatures either caused by slight miscalibration of product or starting material, or potential conversion to unobserved side products.

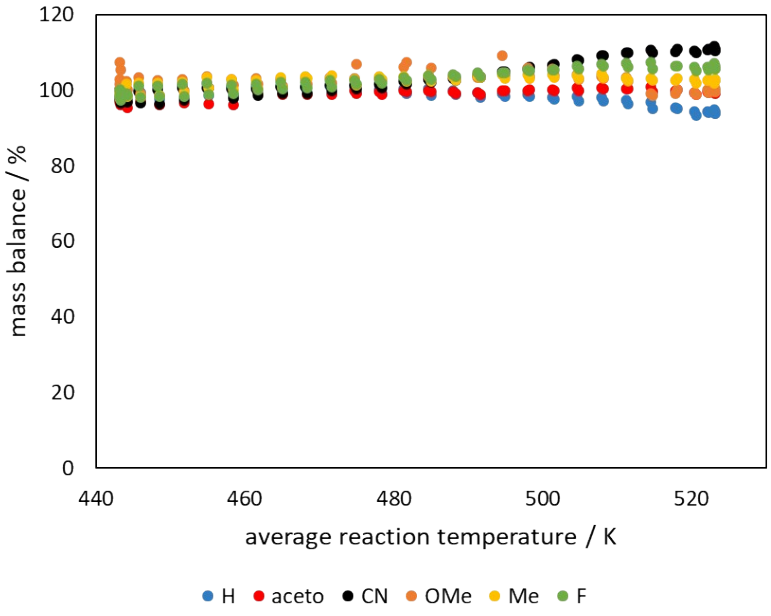

Figure S5. Example mass balance calculations for one of the 170 – 250 – 170 °C one-pot transient temperature ramp experiments used for building the Arrhenius-Hammett plot.

S3.5 Solvent expansion effects on residence time

As previously reported by Noël *et al.* we found that even at high pressures of 100 bar solvent expansion still occurred for ethanol in our temperature range.[9] The residence time at 0.2 mL min^{-1} was calculated to be 19.6 minutes based on the volume of the system. However, when ethanol is heated it expands according to the Tait equation in relation to its bulk modulus and bulk modulus of elasticity. This equation allows calculation of the change in density of ethanol at different temperatures and pressures.

$$\rho_1 = \frac{\rho_0}{1 - \frac{P_1 - P_0}{E}}$$

$$\rho_1 = \frac{\rho_0}{1 + \beta(T_1 - T_2)}$$

Where ρ is the density of ethanol in kg m^{-3}, P is the applied pressure in bar, T is the temperature in K, E is the bulk modulus of elasticity (10600 bar for ethanol), and β is the volumetric expansion coefficient (0.0011 K^{-1} for ethanol).

We found that at 170 °C and 100 bar the corrected residence time would be 16.4 minutes, and at 250 °C and 100 bar it would be 15.1 minutes. This change seemed substantial, so we opted to correct the residence times in calculation of rate constants (k). However, it is worth noting that this correction of residence time has minimal difference on the value of ln(k) as k is calculated to be $(\ln([\mathbf{1}]_0)-\ln([\mathbf{1}]))/\tau$. Thus a change of from 16 to 15 minutes in τ would only cause a ln(16/15) difference in ln(k) which is 0.06 which is insignificant compared to the changes observed in ln(k) with temperature.

S3.6 Comparison of different Hammett parameters

It had previously been reported that the aromatic Claisen rearrangement of *para*-allyl phenyl ethers were best represented by the σ^+ parameter as discussed in the main body. To confirm this was best for our data we compared data taken from a 170 – 250 °C temperature ramp at

190 °C at 0.2 mL min^{-1} (Fig. S6). This clearly showed that the σ^+ parameter was significantly better at representing the trend in relative rates than σ_p, σ_m, and σ^- parameters (R^2 = 0.96 *cf.* 0.79, 0.35, 0.72 respectively).

Table S5. *Para*-substituents (**Z**) for phenyl allyl ether substrates and their corresponding Hammett parameters. σ^+ values were taken from work by McDaniel and Brown.[15] All other σ were taken from a review by Taft *et al.* which also contains the aforementioned σ^+.[16]

1/2	Z	σ^+	σ_p	σ_m	σ^-
a	MeO	-0.78	-0.27	0.12	-0.26
b	Me	-0.31	-0.16	-0.07	-0.17
c	F	-0.07	0.06	0.34	-0.03
d	H	0	0	0	0
e	$C(O)CH_3$	0.50 [a]	0.50	0.38	0.84
f	CN	0.66	0.66	0.56	1.0
g	NHAc	-0.60	0	0.21	-0.46
h	Br	0.15	0.23	0.39	0.25

[a] no σ^+ was available for Z = $C(O)CH_3$ so the σ_p was used.

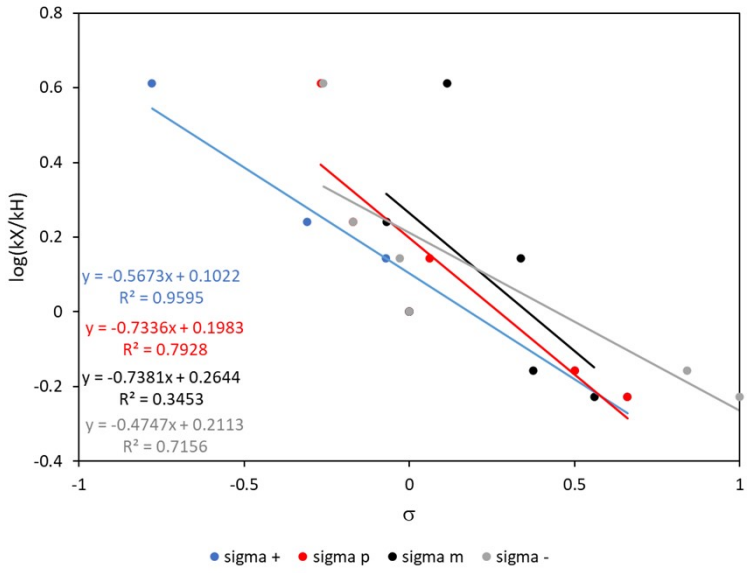

Figure S6. Data collected at 190 °C at 0.2 mL min^{-1} on the aromatic Claisen rearrangement of phenyl allyl ether (**1d**) plotted against a range of Hammett parameters.

S3.7 Observed debromination within the reaction of 1h to 2h

It was observed that in the IS-TF temperature ramps for substrate **1h** (Z = Br) production of the debrominated starting material and product were also observed (**1d** and **2d**) (Fig. S7). The quantity of observed debrominated product were at 250 °C as high as 5%, however generally they were much lower. It is interesting to note that little of the debrominated starting material was observed suggesting that the debromination occurs *after* the rearrangement of the allyl

group.

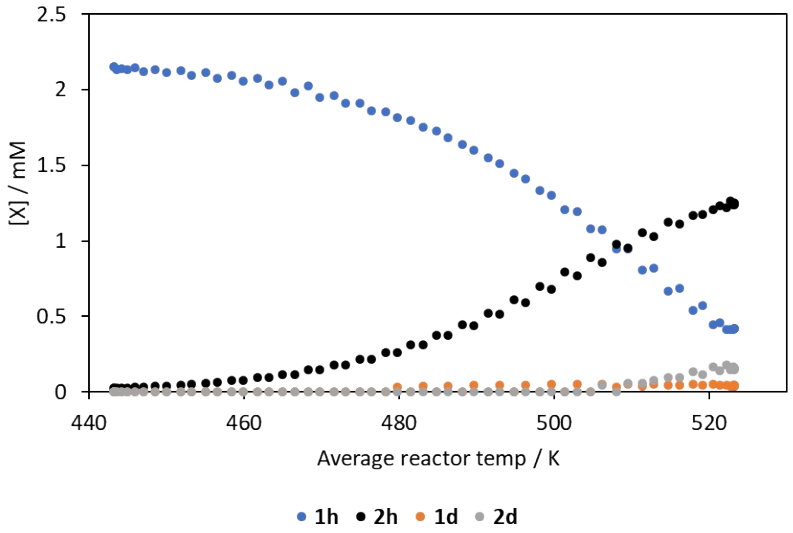

Figure S7. Concentration *vs.* temperature data collected *via* a 170 – 250 – 170 °C transient temperature ramp on **1h** (Z = Br) for the test set data for model prediction. This data shows some debromination leading to the formation of **1d** and **2d**.

S4 Mathematical derivations, code, and data access

S4.1 Mathematical derivation of combined Eyring-Hammett equation

Hammett equation

$$\log\left(\frac{k_X}{k_H}\right) = \rho\sigma^+ \qquad (1)$$

Eyring equation

$$k = \frac{\kappa k_B T}{h} e^{\frac{\Delta S^\ddagger}{R}} e^{-\frac{\Delta H^\ddagger}{RT}} \qquad (2)$$

Conversion to ln from $\log_{10}$ of (1):

$$\log\left(\frac{k_X}{k_H}\right) = \rho\sigma^+ = \frac{1}{\ln(10)} \ln\left(\frac{k_X}{k_H}\right)$$

Differentiating gives:

$$\rho = \frac{1}{\ln(10)} \frac{d(\ln\left(\frac{k_X}{k_H}\right))}{d\sigma^+}$$

Relative rates of the Eyring equation (2) substituting k and simplification gives:

$$\ln\left(\frac{k_X}{k_H}\right) = \ln\left(\frac{\kappa_X}{\kappa_H}\right) + \frac{\Delta S^{\ddagger}_X}{R} - \frac{\Delta S^{\ddagger}_H}{R} - \frac{\Delta H^{\ddagger}_X}{RT} + \frac{\Delta H^{\ddagger}_H}{RT}$$

Generally, κ (transmission coefficient) is assumed to be 1, we have made the weaker assumption that $\kappa_X \approx \kappa_H$. Combining the two above equations by differentiating $\ln\left(\frac{k_X}{k_H}\right)$ by σ^+ gives:

$$\rho = \frac{d}{d\sigma^+}\left(\log\left(\frac{k_X}{k_H}\right)\right) = \frac{1}{R\ ln(10)}\frac{d}{d\sigma^+}\left(\Delta S^{\ddagger}_X\right) - \frac{1}{ln(10)}\frac{d}{d\sigma^+}\left(\Delta H^{\ddagger}_X\right)\frac{1}{RT} \quad (3)$$

Fitting our OF-TF data to an equation of the form

$$\log\left(\frac{k_X}{k_H}\right) = A + B\sigma^+ + C\left(\frac{1}{RT} * 10^3\right) + D\sigma^+\left(\frac{1}{RT} * 10^3\right) + E\left(\frac{1}{RT} * 10^3\right)^2$$

Gives fitting constants with R^2 values of 0.93 (0.95 for repeated experiment). Differentiation of fitted equation leads to an equation in the form of (3), allowing comparison of fitting constants to theoretical equation (bracketed values are calculated from repeated experiment).

$$\frac{1}{R\ ln(10)}\frac{d\Delta S^{\ddagger}}{d\sigma^+} = 1.138\ (1.044)$$

$$\frac{1}{ln(10)}\frac{d\Delta H^{\ddagger}}{d\sigma^+} = 6.648 * 10^3 (6.332 * 10^3)$$

These can be rearranged to produce the values given in the main body of the paper as an average of the two runs.

$$\frac{d\Delta S^{\ddagger}}{d\sigma^+} = 21.79\ (19.99)\ J\ mol^{-1}K^{-1}$$

$$\frac{d\Delta H^{\ddagger}}{d\sigma^+} = 15.31\ (14.58)\ kJ\ mol^{-1}$$

When $\rho = 0, T = \beta$ (isokinetic temperature):

$$T = \beta = \frac{6.490 * 10^3}{1.091\ R} = 715\ K$$

S4.2 Code

All code is available at https://github.com/LindenSchrecker .

The HPLC peak picking, time stamping, and tabulation code for "one-pot" reactions was written in Python based on code from Marvin Alberts.

Arrhenius-Hammett model and thermodynamic values were developed and calculated in

MATLAB.

S5 Supplementary References

1 H. Noda, K. Motokura, A. Miyaji and T. Baba, *Adv. Synth. Catal.*, 2013, **355**, 973–980.

2 A. L. Pincock, J. A. Pincock and R. Stefanova, *J. Am. Chem. Soc.*, 2002, **124**, 9768–9778.

3 Y. Mao, Y. Liu, Y. Hu, L. Wang, S. Zhang and W. Wang, *ACS Catal.*, 2018, **8**, 3016–3020.

4 D. S. Hemming, E. P. Talbot and P. G. Steel, *Tetrahedron Lett.*, 2017, **58**, 17–20.

5 B. Schmidt and F. Wolf, *J. Org. Chem.*, 2017, **82**, 4386–4395.

6 R. Bujok, M. Bieniek, M. Masnyk, A. Michrowska, A. Sarosiek, H. Stępowska, D. Arlt and K. Grela, *J. Org. Chem.*, 2004, **69**, 6894–6896.

7 J. Schlüter, M. Blazejak and L. Hintermann, *ChemCatChem*, 2013, **5**, 3309–3315.

8 J. T. Hutt and J. P. Wolfe, *Org. Chem. Front.*, 2016, **3**, 1314–1318.

9 H. Kobayashi, B. Driessen, D. J. G. P. Van Osch, A. Talla, S. Ookawara, T. Noël and V. Hessel, *Tetrahedron*, 2013, **69**, 2885–2890.

10 Y. Oh, Y. J. Jang, M. Jeon, H. S. Kim, J. H. Kwak, K. H. Chung, S. Pyo, Y. H. Jung and I. S. Kim, *J. Org. Chem.*, 2017, **82**, 11566–11572.

11 H. L. Goering and R. R. Jacobson, *J. Am. Chem. Soc.*, 1958, **80**, 3277–3285.

12 W. N. White, D. Gwynn, R. Schlitt, C. Girard and W. Fife, *J. Am. Chem. Soc.*, 1958, **80**, 3271–3277.

13 L. Schrecker, J. Dickhaut, C. Holtze, P. Staehle, M. Vranceanu, K. Hellgardt and K. K. Hii, *React. Chem. Eng.*, 2022, **8**, 41–46.

14 F. Florit, A. M. K. Nambiar, C. P. Breen, T. F. Jamison and K. F. Jensen, *React. Chem. Eng.*, 2021, **6**, 2306–2314.

15 D. H. McDaniel and H. C. Brown, *J. Org. Chem.*, 1958, **23**, 420–427.

16 C. Hansch, A. Leo and R. W. Taft, *Chem. Rev*, 1991, **91**, 165–195.